Field-free Fast Reliable Deterministic Switching in Perpendicular Spin-Orbit Torque MRAM Cells

Alexander Makarov
Institute for Microelectronics
TU Wien
Wien, Austria
makarov@iue.tuwien.ac.at

Viktor Sverdlov
Institute for Microelectronics
TU Wien
Wien, Austria
sverdlov@iue.tuwien.ac.at

Siegfried Selberherr
Institute for Microelectronics
TU Wien
Wien, Austria
selberherr@tuwien.ac.at

Abstract— **We demonstrate that the spin-orbit torques generated by two orthogonal consecutive current pulses enable reliable and deterministic switching of a perpendicularly magnetized free magnetic layer without applying an external magnetic field. The switching current can be reduced by allowing the wire through which the second pulse is delivered to overlap only partly with the free layer. Surprisingly, the partial overlap makes the switching faster and 100% robust.**

Keywords—spin-orbit torque; MRAM; switching; perpendicularly magnetized MTJ, perpendicular magnetic anisotropy formatting, field-free switching, sub-ns switching

I. INTRODUCTION

The spectacular increase in computational performance of modern integrated circuits is supported by continuing scaling of complementary metal-oxide semiconductor (CMOS) devices, however, a growth of the dynamic and stand-by power becomes a pressing issue [1]. A promising way to slow down this undesirable trend is to introduce non-volatility in the circuits [2]. The development of an electrically addressable non-volatile memory combining high speed, high endurance and long retention is essential to achieve these goals, and spin-transfer torque (STT) magnetoresistive random access memory (MRAM) is a promising candidate of such a memory [3]. It opens a perspective of employing non-volatility in the embedded main computer memory as a replacement of conventional volatile CMOS-based DRAM, which potentially enables an integration of high-performance circuit layers separated by non-volatile memory spacers in three-dimensional monolithic circuits. The availability of high-capacity non-volatile memory close to high-performance CMOS circuits allows exploring conceptually new logic-in-memory [4] and computing-in-memory architectures for future artificial intelligence and cognitive computing [5].

At the same time the large versatility of STT-MRAM with respect to the operation speed makes it a suitable replacement for another type of non-volatile memory, namely flash memory. In fact, all major foundries have announced to start with STT-MRAM production in the current year [6].

To further reduce the energy consumption, it is essential to replace caches (static RAM) in modern hierarchical multi-level processor memory structures with a non-volatile memory technology. Although STT-MRAM can in principle be used in L3 caches [7], the switching current floating through the tunneling oxide becomes very large at an access time of 10ns and faster. This prevents STT-MRAM from entering in L2 and L1 caches currently mastered by static RAM (SRAM). These rapidly increasing critical currents result in large current densities running through the magnetic tunnel junctions (MTJ), worsening the oxide reliability and thus degrading the MRAM endurance to the level of the flash memory.

The development of an electrically addressable non-volatile memory combining sub-ns operation, high endurance, and long retention is thus essential for replacing SRAM in higher-level caches of hierarchical multi-level processor memory structures [4]. Among the newly discovered physical phenomena suitable for next-generation MRAM is spin-orbit torque (SOT) assisted switching at room temperature in heavy metal/ferromagnetic [8-15] or topological insulator/ ferromagnetic [16,17] bilayers. In these memory cells the MTJ's free layer is grown on a material with a large spin Hall angle (heavy metal). By passing the current through the material the SOT acting on the free layer is generated. The large switching current is injected in-plane along the heavy metal line and does not flow through the MTJ. This results in a three-terminal configuration, in which the read and write currents are running through different paths. Now only a weak read current flows through the oxide in MTJ, which does not damage the tunnel barrier.

SOT-MRAM has been proven an electrically addressable non-volatile memory combining high speed, high endurance, and long retention and is thus suitable for applications in caches [14]. Although the high switching current is not flowing through the MTJ, the current is still high, and its reduction is the pressing issue in the field of SOT-MRAM development. Recently, IMEC presented a technology to integrate SOT-MRAM on a 300mm CMOS wafer using CMOS compatible processes [18]. This way the unlimited endurance in SOT-MRAM based on a perpendicular beta-phase W/CoFeB/MgO/CoFeB/synthetic antiferromagnet magnetized stack was achieved.

However, a static magnetic field is still required to guarantee deterministic switching [19]. Several paths to achieve the deterministic switching without magnetic fields were suggested. Though, they require unusual solutions to break the mirror symmetry either by means of shape [20], or by controlling the crystal symmetry of the metal line [13], or by employing exchange coupling to an antiferromagnet [21].
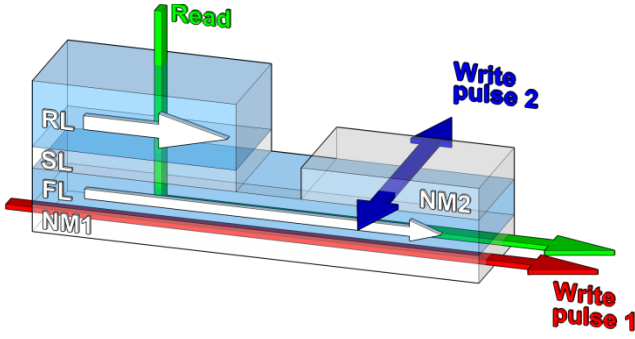
Fig. 1. Scheme of the in-plane SOT-MRAM cell. The free layer of an MTJ is grown above the heavy metal wire NM1, through which the current pulse is applied. The wire NM2 serves to conduct the perpendicular current "Write pulse 2" of the in-plane SOT-MRAM cell.

Fig. 2. Perpendicular SOT-MRAM memory cell with a 52.5nm × 12.5nm × 2nm free layer. After the 100μA/100ps current pulse the second perpendicular pulse is applied.

In this work we propose a switching scheme for a perpendicularly magnetized SOT-MRAM cell based on the use of two consecutive orthogonal sub-nanosecond current pulses [22]. By means of extensive micromagnetic simulations we demonstrate that reliable, deterministic, fast, and magnetic field free switching of the perpendicularly magnetized layers of a rectangular shape is achieved.

II. METHOD

We apply the two-pulse switching scheme previously proposed for efficient switching of an in-plane structure [22] shown in Fig.1. It consists of an in-plane magnetized MTJ with its free layer lying on top of a heavy metal wire NM1 of 3nm thickness. The dimensions of the free layer are 52.5×12.5×2nm^3. Another heavy metal wire NM2 with an overlap from the right side lesser or equal to the total free layer width of 52.5nm serves to apply the second perpendicular current pulse and the spin-orbit torque associated with it. The magnetization dynamics of the magnetic system due to the spin current densities and the spin accumulations is well described by the Landau-Lifshitz-Gilbert equation [23]

$$\frac{\partial \mathbf{m}}{\partial t} = -\gamma \mathbf{m} \times \mathbf{H}_{eff} + \alpha \mathbf{m} \times \frac{\partial \mathbf{m}}{\partial t} + \gamma \frac{\hbar}{2e} \frac{\Theta_{SH} J}{M_0 d} [\mathbf{m} \times (\mathbf{m} \times \mathbf{y})] , \quad (1)$$

where **m** is the position-dependent magnetization **M** normalized by the saturation magnetization M_0: **m**= **M**/M_0, γ is the gyromagnetic ratio, α is the Gilbert damping parameter, e is the electron charge, $\hbar$ is the reduced Plank constant, and Θ_{SH} is an effective Hall angle relating the strength of the spin current density to the charge current density J. If the charge current flows along direction **x** in the heavy metal wire, the spin floats perpendicularly along the **z** direction from the heavy metal to the free ferromagnetic layer of thickness d. The polarization of the spin current is pointing out along the direction **y** perpendicular to both the spin and charge current directions. The spin polarization entering into the free ferromagnetic layer is becoming quickly aligned with the local magnetization **M** generating the torque (the last term in (1)), which acts on the magnetization. This spin-orbit torque together with the magnetic field **H**$_{eff}$ describes the damped magnetization dynamics. The magnetic field **H**$_{eff}$ includes the external field
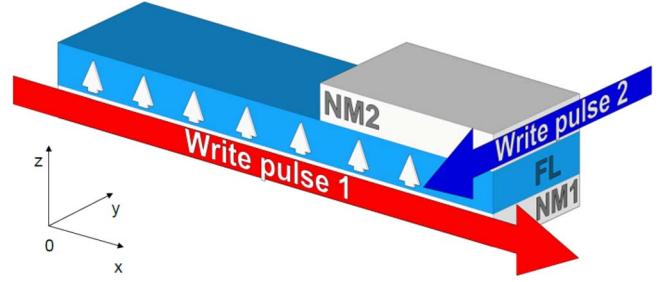
as well as the contributions due to bulk and interface-induced magnetic anisotropies, exchange field, and demagnetization field. Thermal effects on the magnetization dynamics are incorporated by means of a random magnetic field added to **H**$_{eff}$. The strength of the thermal field fluctuations is proportional to temperature [24].

The "Write pulse 1" applied alone does not guarantee the deterministic magnetization switching, and an external magnetic field is required [19]. In contrast, the SOT of the second consecutive pulse through the wire NM2 is able to switch the magnetization deterministically even if it is applied alone [19]. The "Write pulse 2" current is applied along the **y** axis, which results in a torque term similar to the one in (1), where +(-)**y** is replaced with –(+)**x**. However, the SOT due to the "Write pulse 2" is not efficient at the beginning, when the magnetization is along the **x** direction, and a very long incubation time is necessary to develop a substantial deviation of the magnetization from the **x** axis. The role of the "Write pulse 1" is to create this initial magnetization deviation. This deviation in combination with the "Write pulse 2" makes the two-pulse switching very efficient [22].

Now we apply the two-pulse switching scheme to a perpendicularly magnetized layer shown in Fig.2. The current is delivered through the nonmagnetic heavy metal line NM1 and NM2. The free layer dimensions are 52.5nm × 12.5nm × 2nm. The dimensions of NM1 are 3nm thickness × 12.5nm, while the width of NM2 is varying. After 100ps initial thermalization, which produces a slightly different initial magnetization distribution, a 100ps short 100μA current pulse through NM1 is applied. This current density equals 2.6×10^{12} A/m^2 which is only slightly higher than the critical current density 2×10^{12}A/m^2 measured in similar structures [19]. The consecutive perpendicular current pulse of varying strength and duration is applied through NM2. The magnetization dynamics of the magnetic system appears due to the charge current running through the heavy metal wire along the **x** axis and is well described by the Landau-Lifshitz-Gilbert equation (1) with M_0=4×10^{5}A/m and α=0.05. Thermal effects on the magnetization dynamics are described by a fluctuating magnetic field. Different realizations of the field produce diverse realizations of the switching process.
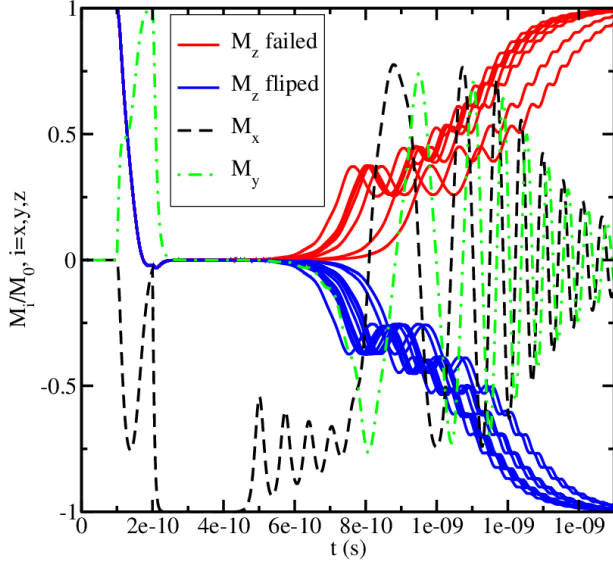
Fig. 3. Time evolution of the magnetization in two-pulse switching (second pulse 1mA/200ps). 20 different switching realizations are obtained after 100ps initial thermalization.

III. RESULTS

The time dependent magnetization dynamics for 20 realizations is shown in Fig.3, where the current density in "Write pulse 2" of 200ps is larger than the critical current applied to NM2 with the width 52.5nm (equal to the free layer width). Although the current is high (1mA), it does not provide a deterministic switching. It orients the magnetization in-plane against the **x** axis, but there is no torque along the **z** axis. Therefore, after the current is turned off, the magnetization randomly relaxes either in the same or in the opposite direction with equal probability because of the perpendicular magnetic anisotropy.
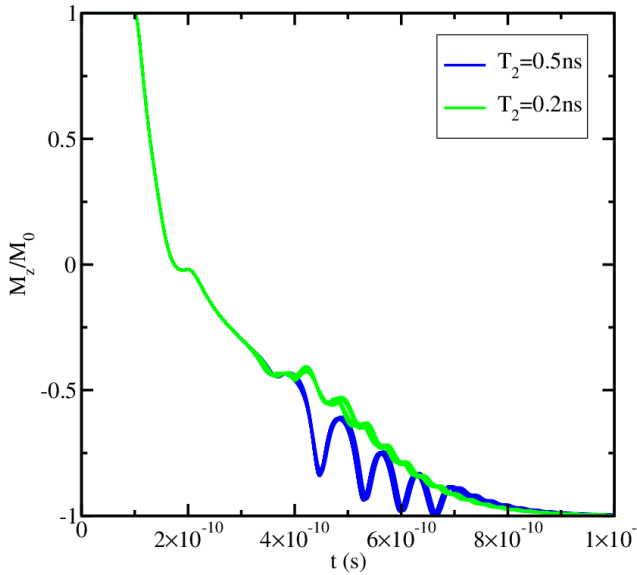

Fig. 5. Randomly chosen switching realizations for the second pulse current of 100μA, for several durations. The switching fails for longer pulses.

Unexpectedly, when the current is reduced to 200μA and the density falls below its critical value, the switching becomes deterministic, for all 20 realizations (Fig.4). In this case the torque due to "Write pulse 2" is not sufficiently strong to align the magnetization along **x** direction and it only tilts the magnetization away from the **y** direction. In this case magnetization precession about the shape effective anisotropy field along the **x** direction, which plays the role of the external field, makes the switching deterministic.

If the current of the "Write pulse 2" is reduced to the value of that in the "Write pulse 1", the switching becomes unreliable, as shown in Fig.5 for several pulse durations.

Fig. 4. Same as in Fig.2, but for the second pulse current of 200μA, for two different durations of the second pulse. The 20 realizations switch evenly, almost without dispersion. The switching is deterministic.
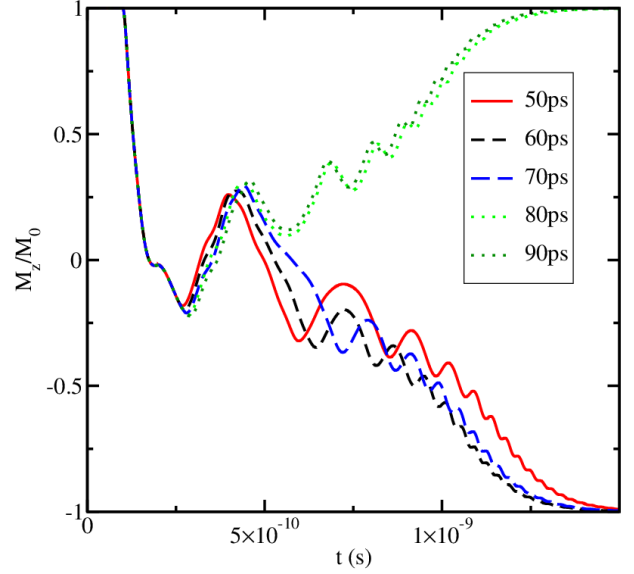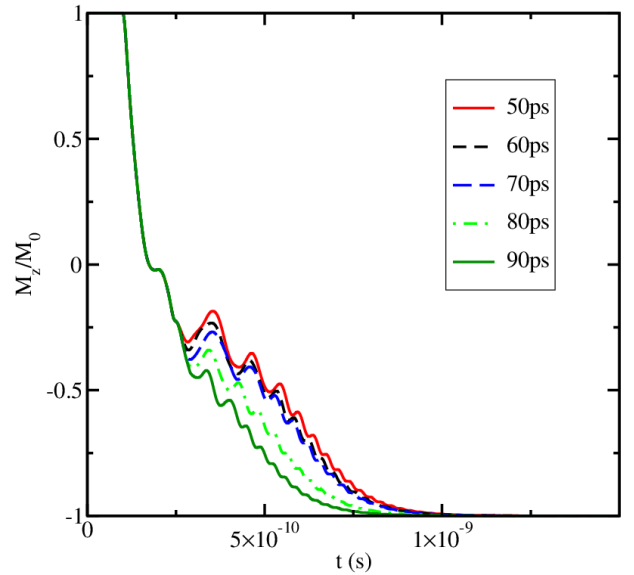

Fig. 6. Same as in Fig.5, but the width of NM2 is 12.5nm (partial overlap). For equal wires NM1 and NM2 and equal currents the switching becomes fast and deterministic.
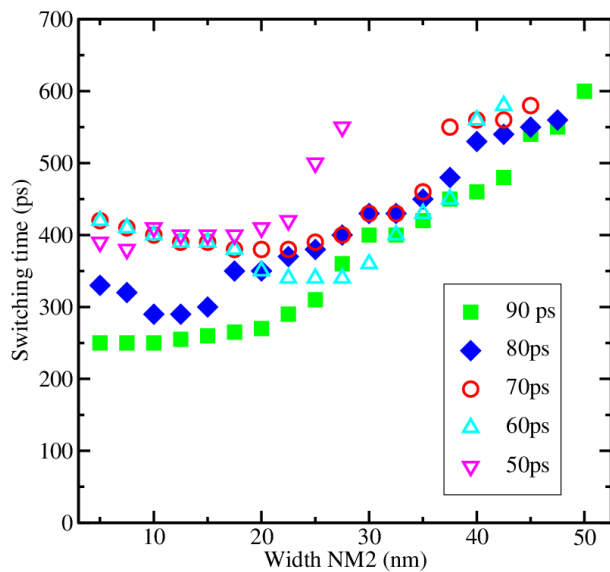
Fig. 7. The switching time as a function of the NM2 width. The NM2 width of 12.5nm is optimal as it guarantees fast, robust, deterministic switching which is insensitive to small variations of the pulse duration or NM2 width.

However, if the width of NM2 is reduced to 12.5nm (width of NM1), the switching becomes deterministic again (Fig.6). In this case the magnetization below NM2 is quickly aligned along the **x** axis. Due to the exchange interaction, the rest of the free layer tilts towards the **x** direction and the anisotropy field acting on it completes the switching deterministically. Fig.7 shows the dependence of the switching time on the NM2 width, for several durations of "Write pulse 2". It appears that the fastest reliable deterministic switching is achieved when the NM2 width is about the same as that of NM1. Most importantly, for these widths the switching is not only fast, but also not very sensitive to the width and pulse duration fluctuations, which relaxes the restrictions for layout and pulse timing.

IV. CONCLUSION

We apply the two-pulse scheme previously proposed for an in-plane structure to switch a perpendicularly magnetized free layer. The spin-orbit torque due to the first 100ps pulse tilts the magnetization of the free layer in-plane perpendicular to the "Write pulse 1" direction. The spin-orbit torque of the second consecutive current "Write pulse 2" results in an additional precession of the magnetization in the part of the free layer under it, which is transferred to the remaining part of the free layer through the exchange interaction. Depending on the direction of this precession, the magnetization of the remaining part tilts up or down with respect to its in-plane orientation set after the "Write pulse 1". The part under the NM2 wire follows the precession after the current is turned off thus completing the switching. Results of the switching time calculations for several pulse durations as a function of the width of the second pulse wire demonstrate that the fastest, sub-300ps, 100% reliable, and magnetic field free switching is achieved at around 30% overlap of the second pulse wire NM2 with the free layer.

REFERENCES

[1] International Roadmap for Devices and Systems (IRDS) 2017 Edition: Executive Summary https://irds.ieee.org/images/files/pdf/2017/2017IRDS_ES.pdf

[2] International Roadmap for Devices and Systems (IRDS) 2017 Edition: Beyond CMOS https://irds.ieee.org/images/files/pdf/2017/2017IRDS_BC.pdf

[3] D. Apalkov, B. Dieny, and J.M. Slaughter, "Magnetoresistive random access memory," *Proceedings of the IEEE*, vol.104, p.1796, 2016.

[4] T. Hanyu, T. Endoh, D. Suzuki *et al.*, "Standby-power-free integrated circuits using MTJ-based VLSI computing," *Proceedings of the IEEE*, vol.104, p.1844, 2016.

[5] D. Ielmini and H.-S.P. Wong, "In-memory computing with resistive switching devices," *Nature Electronics*, vol.1, p.333, 2018.

[6] https://www.mram-info.com/tags/mram_production

[7] G. Jan, L. Thomas, S. Le *et al.*, "Achieving sub‑ns switching of STT‑MRAM for future embedded LLC applications through improvement of nucleation and propagation switching mechanisms," in *Proc.of the 2016 Symp. VLSI Technology and Circuits*, Honolulu, June 13-17 2016, p.18.

[8] I.M. Miron, K. Garello, G. Gaudin *et al.*, "Perpendicular switching of a single ferromagnetic layer induced by in-plane current injection," *Nature*, vol.476, p.189, 2011.

[9] L. Liu , J. Lee, T.J. Gudmundsen *et al.*, "Current-induced switching of perpendicularly magnetized magnetic layers using spin torque from the spin Hall effect," *Phys.Rev.Lett.*, vol.109, 096602, 2012.

[10] L. Liu, C.-F. Pai, Y. Li *et al.*, "Spin-torque switching with the giant spin Hall effect of Tantalum," *Science*, vol.336, p.555, 2012.

[11] A. Brataas and K.M.D. Hals, "Spin–orbit torques in action," *Nature Nanotechnoogy*, vol.9, p.86, 2014.

[12] T. Taniguchi, J. Grollier, and M.D. Stiles, "Spin-transfer torques generated by the anomalous Hall effect and anisotropic magnetoresistance," *Phys.Rev.Appl.*, vol.3, 044001, 2015.

[13] D. MacNeil, G.M. Stiehl, M.H.D. Guimaraes *et al.*, "Control of spin–orbit torques through crystal symmetry in WTe₂/ferromagnet bilayers," *Nature. Physics*, vol.13, p.300, 2017.

[14] S.-W. Lee and K.-J. Lee, "Emerging three-terminal magnetic memory devices," *Proceedings of the IEEE*, vol.104, p.1831, 2016.

[15] K.U. Demasius, T. Phung, W. Zhang *et al.*, "Enhanced spin–orbit torques by oxygen incorporation in tungsten films," Nature Communications, vol.7, 10644, 2016.

[16] J. Han, A. Richardella, S.A. Siddiqui *et al.*, "Room-temperature spin-orbit torque switching induced by a topological insulator," *Phys.Rev.Lett.*, vol.119, 077702, 2017.

[17] Y. Wang, D. Zhu, Y. Wu *et al.*, "Room temperature magnetization switching in topological insulator-ferromagnet heterostructures by spin-orbit torques," *Nature Communications*, vol.8, p.1364, 2017.

[18] K. Garello, F. Yasin, S. Couet *et al.*, "SOT‑MRAM 300mm integration for low power and ultrafast embedded memories," presented at 2018 Symp. VLSI Technology and Circuits, Honolulu, 2018.

[19] S. Fukami, T. Anekawa, C. Zhan, and H. Ohno, "A Spin–orbit torque switching scheme with collinear magnetic easy axis and current configuration," *Nature Nanotechnology*, vol.11, p. 621, 2016.

[20] G. Yu, P. Upadhyaya, Y. Fanet *et al.*, "Switching of perpendicular magnetization by spin-orbit torques in the absence of external magnetic fields," *Nature Nanotechnology*, vol. 9, p.548, 2014.

[21] S. Fukami, C. Zhang, S. Dutta Gupta *et al.*, "Magnetization switching by spin-orbit torque in an antiferromagnet-ferromagnet bilayer system," *Nature Materials*, vol.15, p.535, 2016.

[22] A. Makarov, T. Windbacher, V. Sverdlov, and S. Selberherr, "CMOS-compatible spintronic devices: A review," *Semiconductor Science and Technology*, vol.31, 113006, 2016.

[23] T. Gilbert, "A phenomenological theory of damping in ferromagnetic materials," *IEEE Transactions on Magnetics*, vol.40, p.3443, 2004.

[24] G. Finocchio, M. Carpentieri, B. Azzerboni *et al.*, "Micromagnetic simulations of nanosecond magnetization reversal processes in magnetic nanopillar," *J.Appl.Phys.*, vol.99, 08G522, 2006.